Microstrip Tapped-Line Filter Design

JOSEPH S. WONG, MEMBER, IEEE

Abstract—**The subject of this article is a step-by-step design procedure for microstrip tapped-line filters, accompanied by appropriate design curves. In addition to microstrip tapped-line interdigital filters, a new hairpin-line filter using tapping is introduced. The equation to calculate the singly loaded Q for hairpin resonators produced by tapping is derived. Experimental data is presented for filters over 20-percent bandwidth.**

I. Introduction

TAPPED-LINE filters have been described by several authors [1]–[3]. The schematic diagrams of the two common types are depicted in Figs. 1(a) and (b).

Tapped-line filters offer space and cost-saving advantages over conventional filter types (in which input/output end sections are parallel coupled to the first and last resonators) because the first and the last end sections of the filter are eliminated. A further benefit is derived in situations where the parallel coupling at the end sections becomes very tight and physical realization becomes impractical; the same filter can still be realized by tapping. Unfortunately, exact designs of tapped-line filters are not simple, and the techniques available are not directly applicable to microstrip configurations. Among the presently available tapped-line designs, although Dishal's method [1] is approximate, it is more straightforward to design. The purpose of this paper is to follow Dishal's method to generate design data which can be used directly to design microstrip tapped-line filters. The microstrip tapped-line filters presented herein are restricted to the interdigital filters illustrated in Fig. 1(a) and the hairpin-line filters shown in Fig. 2. The equation to calculate the singly loaded Q produced by tapping a hairpin resonator is derived. Step-by-step filter design procedures, design curves, and experimental results of the sample filters are presented.

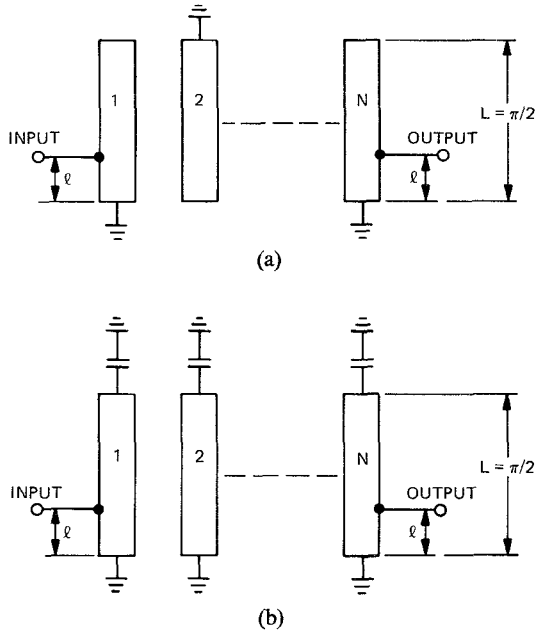

Fig. 1. Tapped-line filters: (a) interdigital and (b) combline.

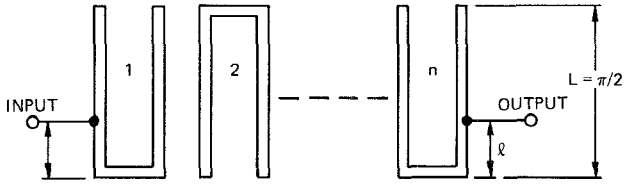

Fig. 2. Tapped-line hairpin-line filter.

II. Microstrip Tapped Interdigital Filter Design

In microstrip tapped interdigital filter designs, the required parameters are the singly loaded $Q(Q_s)$ of the first and the last resonators produced by tapping and the coupling coefficient (K) between the adjacent resonators. Once the singly loaded Q is known, the tap point l/L of Fig. 1(a) can be calculated from

$$\frac{Q_{si}}{(R/Z_0)} = \frac{\pi}{4\sin^2\frac{\pi l}{2L}} \tag{1}$$

where R is the generator impedance and Z_0 is the filter internal impedance. The coupling coefficients (K's) can be experimentally determined using Dishal's [4] procedure to determine the unloaded Q and the coupling coefficient (K) of a pair of resonators. This method is depicted in Fig. 3 and can be used for this microstrip filter. As shown in Fig. 3, the generator at the input is capacitively coupled (loosely) to the open-circuit end of the same resonator. When both ends of resonator 2 are short-circuited, resonator 1 alone is a single-tuned circuit. The response curve is depicted in Fig. 4(a). The unloaded $Q(Q_0)$ is related as

$$Q_0 = \frac{\Delta f}{f_0} \tag{2}$$

Manuscript received October 21, 1977; revised August 21, 1978.

The author is with the International Telephone and Telegraph Corporation, Avionics Division, Aerospace, Electronics, Components, and Energy Group, Nutley, NJ 07110.

0018-9480/79/0100-0044$00.75 ©1979 IEEE

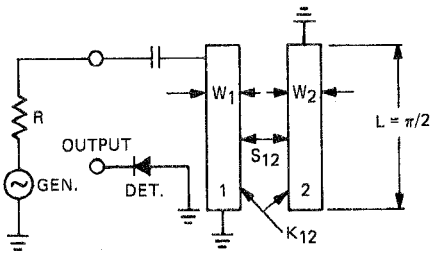

Fig. 3. Measurement of coupling coefficients.

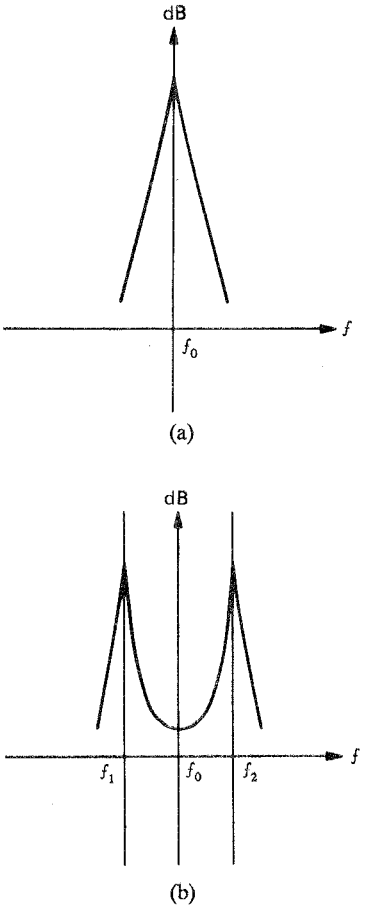

Fig. 4. Circuit responses: (a) single-tuned circuit response and (b) double-tuned circuit response.

where Δf is the 3-dB bandwidth. If one end of resonator 2 is open-circuited as indicated in Fig. 3, the pair of resonators becomes a double-tuned circuit. The response curve is presented in Fig. 4(b). The coupling coefficient (K) of the pair of resonators is related as

$$K = \frac{f_2 - f_1}{f_0}. \tag{3}$$

The coupling coefficient (K) determined from this experiment is based on the stripwidths (W_1; W_2) and spacing (S_{12}) between the resonators. In Dishal's method, the stripwidth of each resonator can be selected to be equal, and the spacings are varied to obtain various couplings. As shown in Fig. 5, for each pair of resonators selected, a

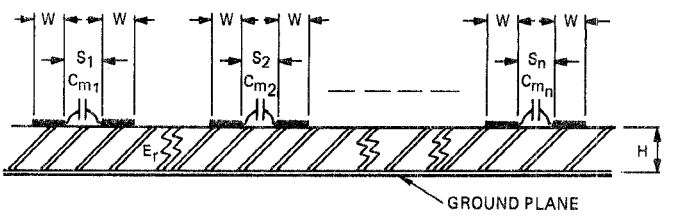

Fig. 5. Pairs of resonators for determining various coupling coefficients.

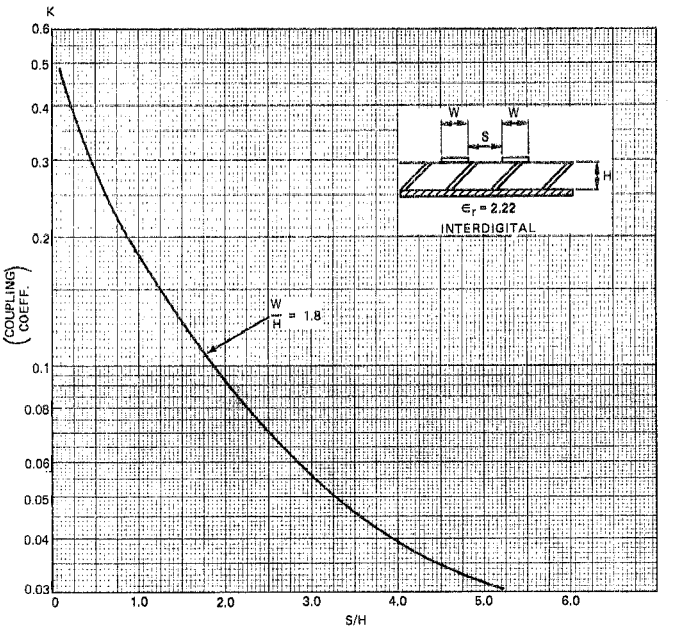

Fig. 6. Experimental design curve for tapped interdigital filters.

point with S/H as a function of $K(S/H,K)$ can be obtained. Thus, by selecting a number of pairs of resonators with physically realizable gaps between each pair (ranging from very narrow to very wide), a curve of S/H as a function of K can be experimentally obtained. The design curve of Fig. 6 is determined in this manner for $\epsilon_r = 2.22$ (#5880 Duroid, Rogers Corp.) and $W/H = 1.8$, which corresponds to a single-strip impedance of approximately 70 Ω. (The choice of this strip impedance is based on the fact that a 70-Ω filter internal impedance has been commonly used.) From the design curve, any filter having this ϵ_r and W/H with coupling coefficients within the range depicted in Fig. 6 can be designed. A typical example of a step-by-step microstrip interdigital filter design by tapping is described in the following paragraphs.

The filter specification is 8 poles, 0.1-dB Chebyshev ripple, and 25-percent bandwidth passing frequencies from 950 to 1225 MHz. The filter to be designed is illustrated schematically in Fig. 7. The first step in designing this filter is to determine its 3-dB bandwidth. Since the passband bandwidth is 275 MHz, centering at 1087.5 MHz [5, pp. 8–12], the 3-dB bandwidth is determined to be 288 MHz from curve no. 5 using the relationship $BW_{3\,dB} = BW/0.955$. For maximum-power-transfer terminations, the normalized singly loaded q's and the normalized cou-

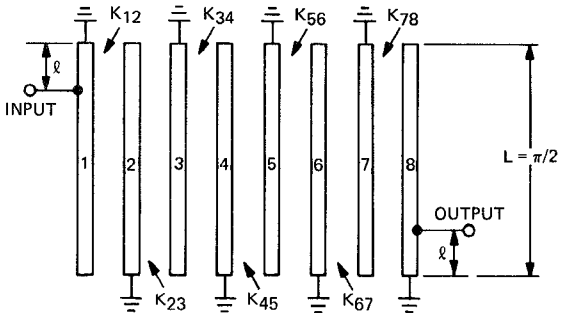

Fig. 7. Eight-pole microstrip tapped-line interdigital filters.

TABLE I
DIMENSIONS FOR SAMPLE FILTERS

Filter No. 1 (BW=25%)		Filter No. 2 (BW=32%)		Filter No. 3 (BW=25%)	
#5880 Duroid		99.5 percent Alumina		99.5 percent alumina	
Interdigital		Interdigital		Hairpin	
L = 50.597 mm		L = 27.330 mm		L = 29.210 mm	
H = 1.575 mm		H = 1.270 mm		H = 1.270 mm	
W = 2.845 mm		W = 0.889 mm		W = 0.889 mm	
W_o = 4.572 mm(50Ω)		W_o = 1.270 mm(50Ω)		W_o = 1.270 mm(50Ω)	
K	S(mm)	K	S(mm)	K	S(mm)
0.193	1.397	0.244	0.762	0.196	0.127
0.144	2.032	0.183	1.092	0.148	0.305
0.137	2.134	0.173	1.143	0.142	0.381
0.135	2.184	0.171	1.168	0.148	0.305
0.137	2.134	0.173	1.143	0.196	0.127
0.144	2.032	0.183	1.092		
0.193	1.397	0.244	0.762		

pling coefficients (k's) for this filter are provided in [5, Table VII, pp. 8–28]. They are

$$q_{2,3,4,5,6,7} = \infty$$
$$q_1 = q_8 = 1.25$$
$$k_{12} = k_{78} = 0.727$$
$$k_{23} = k_{67} = 0.545$$
$$k_{34} = k_{56} = 0.516$$
$$k_{45} = 0.510.$$

The actual coupling coefficients (K's) of the filter can be computed from the expression [1]

$$K = k\left(\frac{BW_{3\,\mathrm{dB}}}{f_0}\right). \tag{4}$$

The physical dimensions of the filter (filter no. 1) are summarized in Table I. The final step is to calculate the input and output tap-point locations (l/L). By using (1) together with the following relationship [1],

$$Q_s = q\left(\frac{f_0}{BW_{3\,\mathrm{dB}}}\right) \tag{5}$$

l/L can be determined. For a 50-Ω (R=50-Ω) generator impedance and 70-Ω (Z_0=70-Ω) filter internal impedance, l/L is calculated to be 0.223 or l=11.278 mm. The l/L can also be calculated from the graph plotted in Fig. 8, which is the extension of [1, Fig. 2].

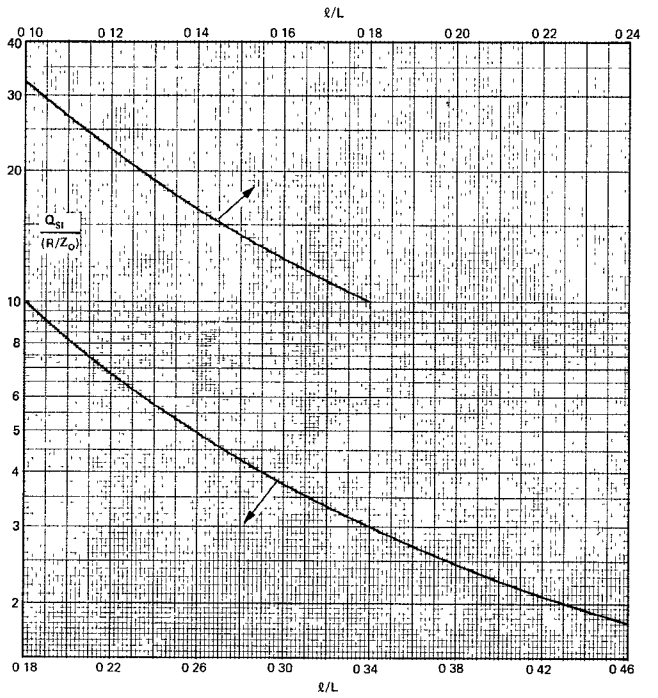

Fig. 8. Singly loaded Q for tapped interdigital resonator.

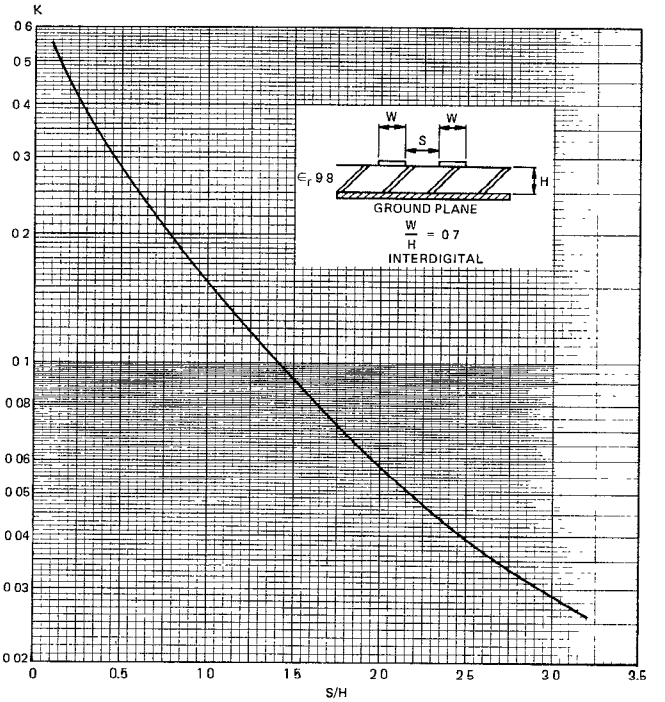

Fig. 9. Experimental design curve (interdigital).

A second filter (filter no. 2) of the same specifications except that the bandwidth is increased to 32 percent has been designed on a 1.270-mm thick 99.5-percent alumina substrate (ϵ_r=9.8) by using the design curve presented in Fig. 9. The dimensions of this filter can be determined by following the same procedure and are summarized in Table I. For R=50 Ω and Z_0=58 Ω selected for the filter,

the tap-point location (l/L) is calculated to be 0.280 from Fig. 8, or $l=7.645$ mm. Z_0 is selected to be 58 Ω in alumina instead of the usual 70 Ω for the filter design because the strip width of 70 Ω in alumina becomes relatively narrow, which normally increases the loss; therefore, a lower impedance line is more practical for loss consideration.

III. Microstrip Tapped Hairpin-Line Filter Design

To this author's knowledge, tapped hairpin-line filters have not appeared in any literature. The design of this type of filter is similar to that previously described for tapped interdigital filters. The design curve can be generated in the same manner as described previously; a typical design curve is depicted in Fig. 10. The advantage of this design is that when the coupling at the end sections of the conventional hairpin-line filters described in [6] and [7] becomes too tight, the tapped transformer realization becomes more practical.

Since hairpin resonators are open-circuited at both ends and are one-half wavelength long, the equation to calculate the singly loaded Q of such a resonator produced by tapping is different from that of the interdigital resonator. Consequently, (1) is not valid in this case. The simple derivation of the singly loaded Q of a tapped hairpin resonator is described in the following paragraphs.

A tapped hairpin resonator is schematically depicted in Fig. 11. Assuming the coupling between the two arms of the resonator is minimum and negligible, its equivalent circuit is depicted in Fig. 12. In [5, pp. 24–14, 15], it can be demonstrated that, near resonance, the input admittance of Fig. 12 at the tap point is

$$Y=G+jB=\frac{\pi Y_0}{2\sin^2\theta_1}\left(\frac{1}{Q_{sh}}+j_2\frac{f-f_0}{f_0}\right) \tag{6}$$

provided that

$$\left|\frac{f-f_0}{f_0}\right|\ll 1.0$$

and

$$\left[\frac{\theta(f-f_0)}{f_0}\right]\cot\theta_1\ll 1.0.$$

By equating the real parts of (6), the singly loaded Q is obtained and is defined as

$$Q_{sh}=\frac{R}{Z_0}\frac{\pi}{2\sin^2\theta_1} \tag{7}$$

or

$$\frac{Q_{sh}}{(R/Z_0)}=\frac{\pi}{2\sin^2\left(\frac{\pi l}{2L}\right)}.$$

By comparing (7) and (1) notice that the singly loaded Q of a tapped interdigital resonator and a tapped hairpin resonator are different by a factor of 2; for convenience, $Q_{sh}/(R/Z_0)$ of (7) is plotted as a function of l/L in Fig. 13.

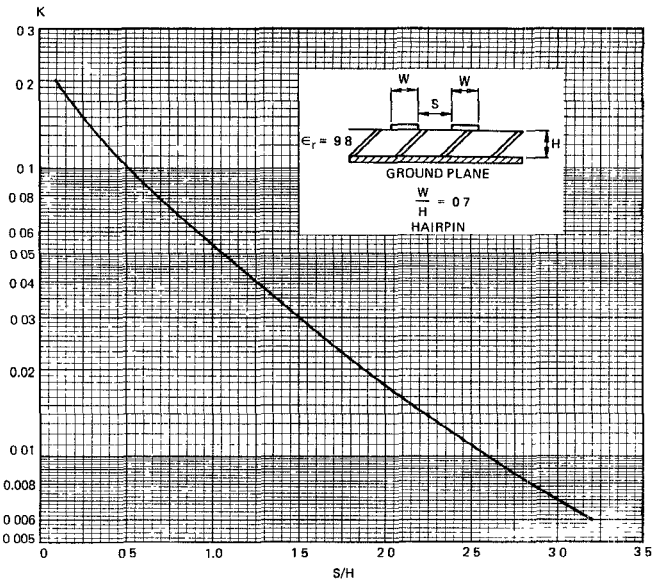

Fig. 10. Experimental design curve (hairpin).

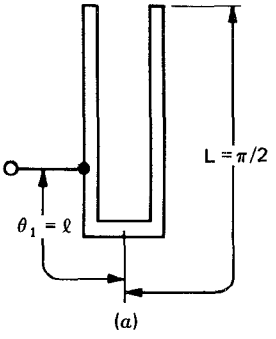

(a)

Fig. 11. Tapped hairpin resonator, schematic diagram.

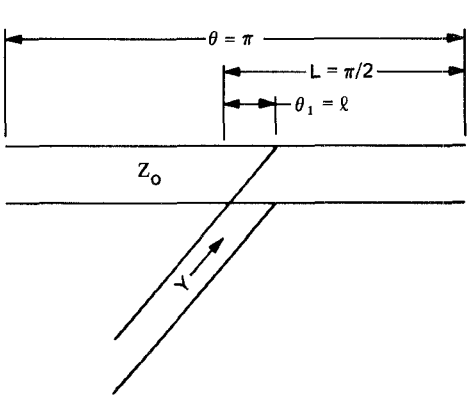

Fig. 12. Equivalent circuit of a tapped hairpin resonator.

The following design example is pertinent for a 6-pole 0.1-dB ripple Chebyshev response tapped hairpin-line filter (filter no. 3). The passband is the same as the first sample filter except $BW/BW_{3\ dB}$ is 0.922 for 6-pole instead of 0.955. The diagram of this filter is illustrated in Fig. 14. The following normalized end q's and the normal-

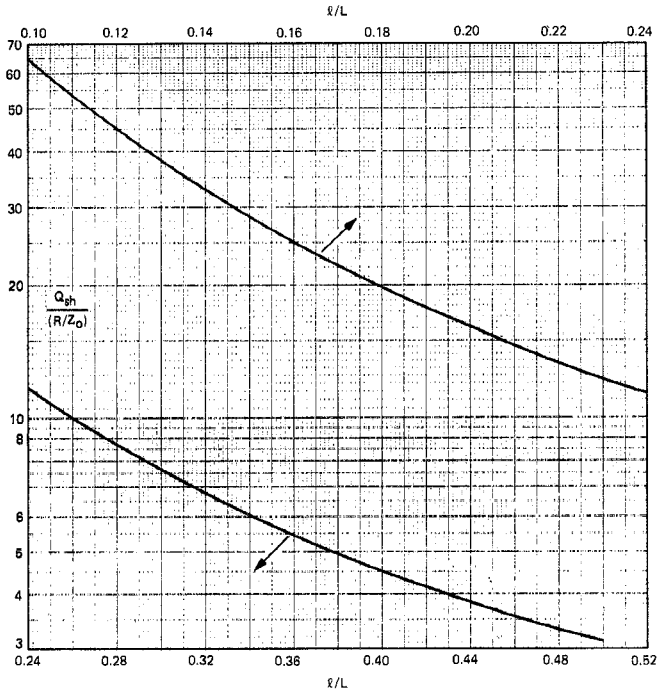

Fig. 13. Singly loaded Q for tapped hairpin resonator.

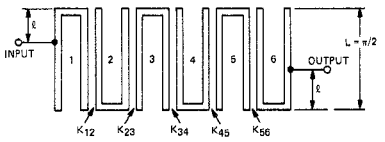

Fig. 14. 6-pole tapped hairpin-line filter.

ized k's for the 6-pole 0.1-dB ripple filter are found in [5, pp. 8–27]:

$$q_2, 3, 4, 5 = \infty$$
$$q_1 = q_6 = 1.27$$
$$k_{12} = k_{56} = 0.716$$
$$k_{23} = k_{45} = 0.539$$
$$k_{34} = 0.518.$$

The filter dimensions for a 1.270-mm thick alumina substrate are obtained from Fig. 10 and summarized in Table I. For $R = 50\ \Omega$ and $Z_0 = 58\ \Omega$, (the single-strip impedance selected for the hairpin resonator) the tap point location (l/L) is calculated to be 0.364 (Fig. 13) or $l = 10.643$ mm. The spacing between the two arms of the hairpin resonator is set at 1.106 mm which is approximately 16 dB of coupling. This coupling is not included in the design.

IV. Design Analysis and Experimental Results

In the present experimental filter design, one advantage is the ability to set all the filter resonators to equal line width with spacing S/H ratio as the single variable. On alumina, the line width is based on a filter impedance of 58 Ω, and on Duroid it is based on 70 Ω. For those designers who wish to select other impedance levels for specific requirements, the technique for generation of the design curves has already been available.

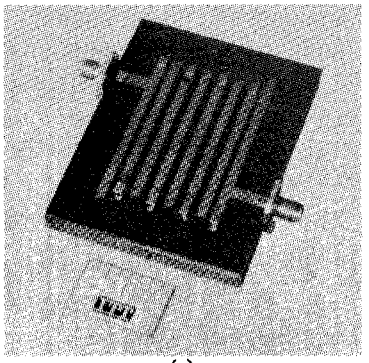

(a)

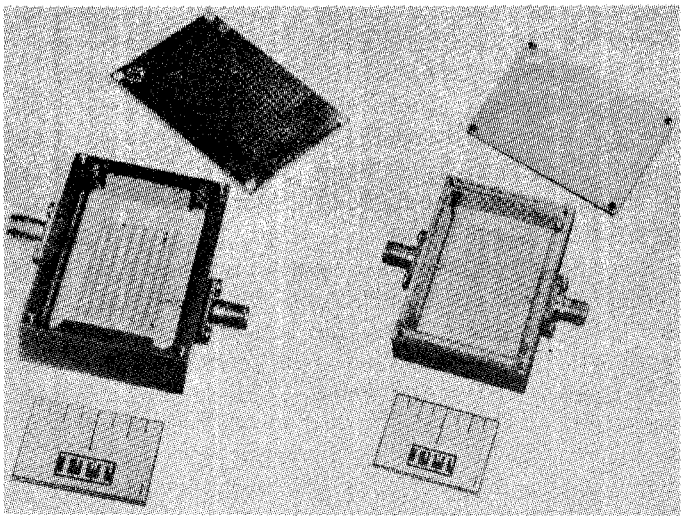

(b) (c)

Fig. 15. Representative microstrip tapped-line filters: (a) filter no. 1, (b) filter no. 2, and (c) filter no. 3.

Based on the empirical design curves illustrated in Figs. 6, 9, and 10 the author has designed, tested, and evaluated a variety of filters. The three filters listed in Table I are the more representative ones among those designed. Their results are presented and analyzed in the following paragraphs.

Filter no. 1 is fabricated on a 76.2 mm by 58.42 mm by 1.575 mm no. 5880 Duroid substrate. Both filter no. 2 and filter no. 3 are fabricated on a 38.10 mm by 25.40 mm by 1.27 mm 99.5-percent alumina substrate. Photographs of the three sample filters are presented in Figs. 15(a), (b), and (c), respectively.

Since the design of the tapped-line filter is based on the selection of the physical parameters together with the empirical data compiled on a limited number of points over the frequency band of interest, some adjustment is usually required on these filters during the bench testing. For the interdigital filter, the adjustment can be performed in two steps.

1) Increase the input/output resonator lengths by approximately 10 percent of the quarter wavelength calculated at the center frequency during the design. A 5-percent increase is usually the required length in L band, and the other five percent is usually trimmed off during the adjustment. This lengthening of the input/output resonators is performed to compensate for the effect of the

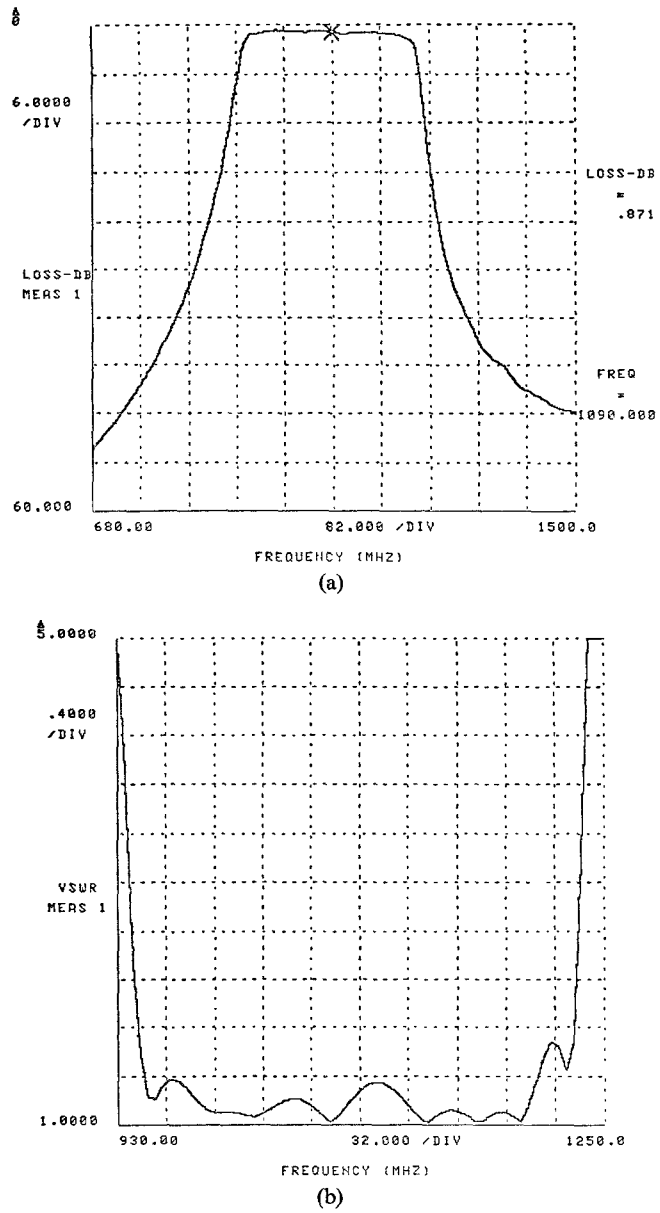

Fig. 16. Filter no. 1 responses: (a) passband response and (b) VSWR response.

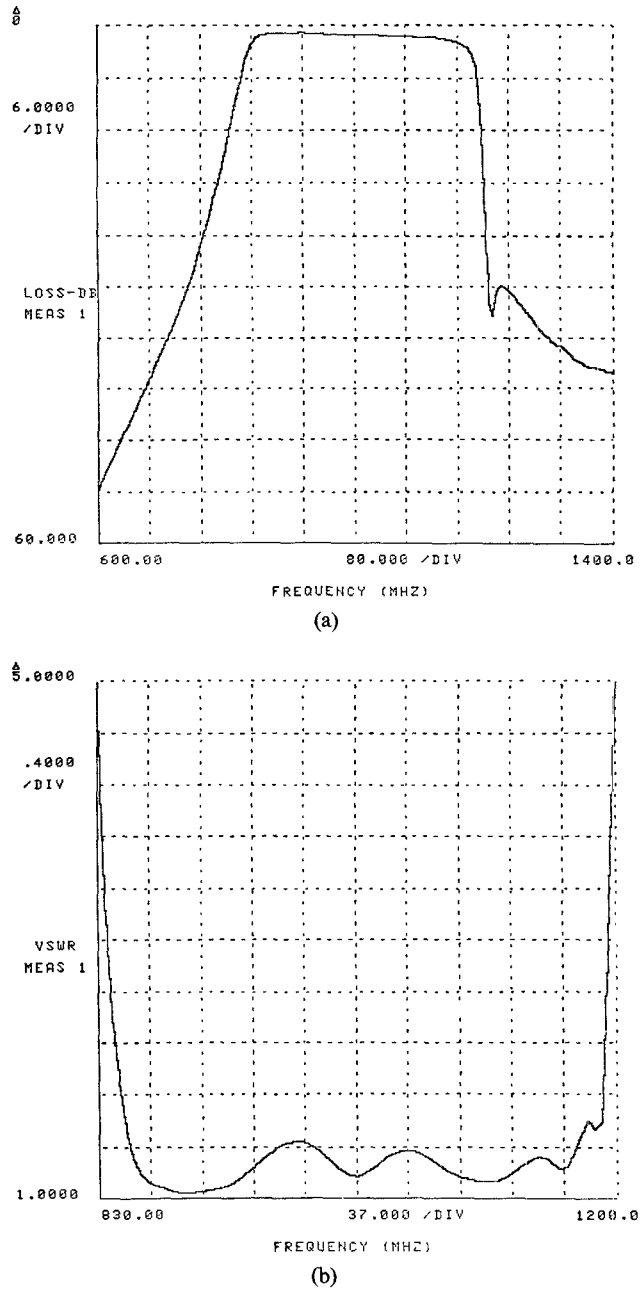

Fig. 17. Filter no. 2 responses: (a) passband response and (b) VSWR response.

physical tap-point 50-Ω loading and serves two purposes: to obtain a correct length at the resonant frequency and to experimentally correct tap-point location. During bench tests, gradually trim the input/output resonators at the open end until both input/output VSWR has reached the optimum achievable equal ripple performance across the band.

2) Minimize the input/output VSWR by adding a small tuning stub at the input/output 50-Ω transmission line. In this way, the best overall filter performance can be achieved.

The previously described step adjustments are determined to be sufficient, and no spacing adjustment is necessary between the resonators; therefore, no adjustment is made to the internal resonators of the filters.

For the hairpin-line filter, the input/output resonators did not require lengthening; however, the tap-point location (l/L) must be increased by approximately the amount of the gap distance between the two arms of the resonator from the calculated value. The first adjustment on the bench is to shorten the gap in small amounts lengthwise at the "U" with a piece of indium foil until equal ripple VSWR is achieved. The next step is to minimize the VSWR according to the procedure described in step 2 for the interdigital filter.

In production of both interdigital and hairpin-line filters, the adjustment from the prototype may be incorporated into the artwork as part of the design. The passband and VSWR response illustrated in Figs. 16–18 are achieved after the three sample filters have been adjusted. By comparison, the results of these three microstrip filters are much better than those reported by Milligan [8].

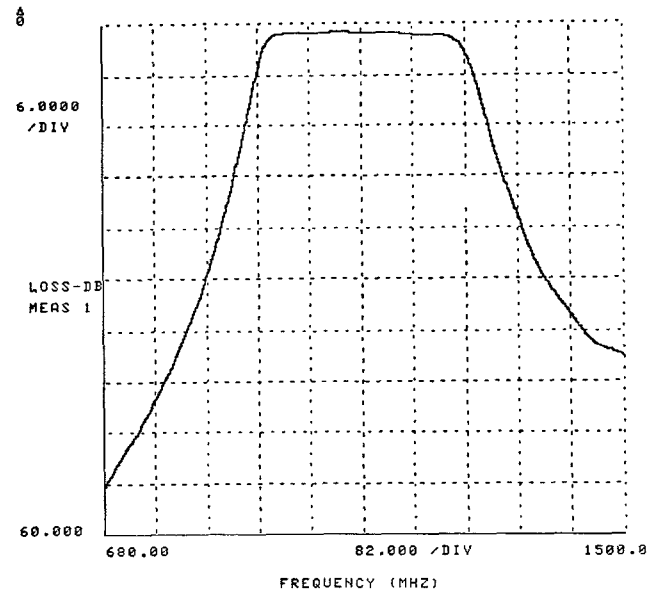

(a)

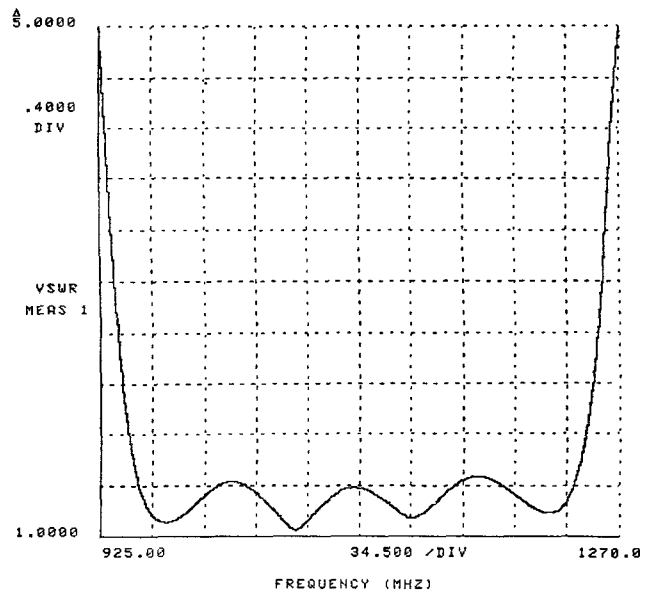

(b)

Fig. 18. Filter no. 3 responses: (a) passband response and (b) VSWR response.

V. Conclusions

A technique to design microstrip tapped-line filters has been presented. The effectiveness of this design has been proven by the experimental results of the sample filters. The performance of this type of microstrip filter appears to be more predictable than that of previously reported filters. The obtainable bandwidth is also wider in the microstrip geometry. Although the coupling coefficient data is obtained from the two-line coupling geometry, the error seems to be negligible when applied to multiconductor geometry for L-band frequencies because the coupling coefficients derived from the experimental curves do not require correction to obtain appropriate resonator spacings. However, this fact may not be true at much higher frequencies. In reference to the design curve depicted in Fig. 6, since the coupling coefficient data was obtained for an open microstrip configuration (top ground plane not included), some scaling of the coupling coefficients is required if the filter is to be operated in the enclosed case for which air-space height is less than ten times the thickness of the substrate thickness. In the enclosed case, the coupling coefficients are tighter than the open geometry for the same filter bandwidth. The author found that this scaling is most effectively accomplished by building a trial filter and then scaling the coupling coefficients proportional to the bandwidth shrinkage. Another approach is to obtain a new set of data for the exact enclosure of the filter, especially if the designer is working in the considerably higher frequency range. The coupling coefficient data presented in Figs. 9 and 10 was obtained in the enclosed case of air-space height equal to eight times the substrate thickness.

The advantage of the microstrip tapped-line filter design over the conventional microstrip filter design is that for moderate bandwidth (over 20 percent), the tapped-line microstrip filter can still be easily realized physically, whereas the conventional microstrip filter has already reached its physical limit. The disadvantage of this design is that at very high frequency, the tap-point loading junction becomes considerable compared to the wavelength, and this loading may not be practical. For very narrow band design (5 percent or less), the distance from tap-point location (l/L) to the short becomes very small. In this case, use of the conventional design is advantageous. Although the tapped-line microstrip filter has its own shortcoming, it has certainly filled the gap where other types of microstrip filters are not achievable.

Acknowledgment

The author wishes to thank G. Scherer and V. Hazners for their constant encouragement, M. Dishal for fruitful technical discussions, and the reviewers for their constructive criticism.

References

[1] M. Dishal, "A simple design procedure for small percentage bandwidth round-rod interdigital filters," *IEEE Trans. Microwave Theory Tech.*, vol. MTT-13, pp. 696–698, Sept. 1965.

[2] S. B. Cohn, "Generalized design of bandpass and other filters by computer optimization," in *1974 IEEE Int. Microwave Symp. Dig. Tech. Papers*, pp. 272–273 (IEEE Catalog no. 74CH0838—3 MTT).

[3] E. G. Cristal, "Tapped-line coupled transmission lines with applications to interdigital and combline filters," *IEEE Trans. Microwave Theory Tech.*, vol. MTT-23, pp. 1007–1012, Dec. 1975.

[4] M. Dishal, "Alignment and adjustment of synchronously tuned multiple-resonant-circuit filters," *Proc. IRE.* vol. 39, pp. 1448–1455, Nov. 1951.

[5] International Telephone and Telegraph Corp., *Reference Data for Radio Engineers*, 6th Ed. Howard W. Sams Co., Inc.

[6] E. G. Cristal and S. Frankel, "Hairpin-line and hybrid hairpin-line /half-wave parallel-coupled-line filters," *IEEE Trans. Microwave Theory Tech.*, vol. MTT-20, pp. 719–728, Nov. 1972.

[7] U. H. Gysel, "New theory and design for hairpin-line filters," *IEEE Trans. Microwave Theory Tech.*, vol. MTT-20, pp. 523–531, May 1974.

[8] T. A. Milligan, "Dimensions of microstrip coupled lines and interdigital structures," *IEEE Trans. Microwave Theory Tech.*, vol. MTT-25, pp. 405–410, May 1977.